Computing adjoint-weighted kinetics parameters in Tripoli-4 by the Iterated Fission Probability method

Guillaume Truchet, Pierre Leconte, Alain Santamarina, Emeric Brun, Zohia
Andrea

Computing adjoint-weighted kinetics parameters in Tripoli-4 ® by the Iterated Fission Probability method

Guillaume Truchet[a], Pierre Leconte[a], Alain Santamarina[a], Emeric Brun[b], Andrea Zoia[b,*]

[a]CEA, DEN, DER/SPRC, Cadarache
F-13108 Saint Paul Lez Durance, FRANCE.
[b]CEA, DEN, DM2S/SERMA/LTSD, Saclay
91191 Gif-sur-Yvette, FRANCE.

Abstract

The analysis of neutron kinetics relies on the knowledge of adjoint-weighted kinetics parameters, which are key to safety issues in the context of transient or accidental reactor behavior. The Iterated Fission Probability (IFP) method allows the adjoint-weighted mean generation time and delayed neutron fraction to be computed within a Monte Carlo power iteration calculation. In this work we describe the specific features of the implementation of the IFP algorithm in the reference Monte Carlo code Tripoli-4 ® developed at CEA. Several verification and validation tests are discussed, and the impact of nuclear data libraries, IFP cycle length and inter-cycle correlations are analyzed in detail.

Keywords: Iterated Fission Probability, Kinetics parameters, Monte Carlo, Tripoli-4 ®

1. Introduction

Knowledge of kinetics parameters is key to the study of nuclear reactor dynamics, in connection with transient behavior due to normal operation or accidents (Bell and Glasstone, 1970; Keepin, 1965). Usually, kinetics parameters stem from integrating the full time-dependent Boltzmann and precursors equations over the space, energy and angle variables: after various algebraic manipulations, they take the general form of a ratio of dot products, namely, $\langle \psi, F\varphi \rangle / \langle \psi, G\varphi \rangle$, where F and G are operators acting on the neutron flux φ, and ψ is a weighting function depending on specific choices associated to the system under analysis (Bell and Glasstone, 1970; Keepin, 1965; Ott and Neuhold, 1985; Henry, 1958; Cohen, 1958). Essential to reactor control are the mean generation time of a neutron within a reactor, which is expressed as

$$\frac{\langle \psi, \frac{1}{v}\varphi \rangle}{\langle \psi, P\varphi \rangle}, \tag{1}$$

where P is the total fission operator (including prompt and delayed productions) and v is the neutron speed; and the delayed neutron fraction, which is expressed as

$$\frac{\langle \psi, B\varphi \rangle}{\langle \psi, P\varphi \rangle}, \tag{2}$$

where B is the fission operator corresponding to delayed neutrons alone (Bell and Glasstone, 1970; Keepin, 1965). Most often, the weighting function ψ is either taken to be $\psi = 1$, in

which case the kinetics parameters are said to be un-weighted, i.e.,

$$\Lambda_0 = \frac{\langle 1, \frac{1}{v}\varphi \rangle}{\langle 1, P\varphi \rangle}, \quad \beta_0 = \frac{\langle 1, B\varphi \rangle}{\langle 1, P\varphi \rangle} \tag{3}$$

or $\psi = \varphi^\dagger$ ($\varphi^\dagger$ denoting the adjoint neutron flux), in which case the kinetics parameters are said to be adjoint-weighted, or effective, namely,

$$\Lambda_{\text{eff}} = \frac{\langle \varphi^\dagger, \frac{1}{v}\varphi \rangle}{\langle \varphi^\dagger, P\varphi \rangle}, \quad \beta_{\text{eff}} = \frac{\langle \varphi^\dagger, B\varphi \rangle}{\langle \varphi^\dagger, P\varphi \rangle}. \tag{4}$$

In the context of reactor physics, Monte Carlo simulation is considered as the gold standard for the computation of physical quantities and is traditionally adopted so as to establish reference values for faster, but approximated, deterministic calculations (Spanier and Gelbard, 1969; Bell and Glasstone, 1970). Monte Carlo codes are intrinsically based on the simulation of forward random walks, with particles flowing from birth (fission) to death (spatial leakage or absorption): as such, they are ideally suited to provide accurate estimates of the direct flux φ and more generally of physical observables weighted by φ. Un-weighted kinetics parameters can be straightforwardly obtained by running standard (forward) criticality simulations (Spriggs et al., 1997) and following their precise definition in Eq. (3). For instance, the mean generation time Λ_0 can be estimated by recording the neutron flight time from birth to fission, and the mean delayed neutron fraction β_0 can be estimated by recording the fraction of delayed neutrons emitted at fission (Spriggs et al., 1997). The so-called removal time

$$T_0 = \frac{\langle 1, \frac{1}{v}\varphi \rangle}{\langle 1, L\varphi \rangle} = k_{\text{eff}}\Lambda_0, \tag{5}$$

---

*Corresponding author. Tel. +33 (0)1 69 08 95 44
Email address:* andrea.zoia@cea.fr (Andrea Zoia)

where L is the net disappearance operator and k_{eff} is the effective multiplication factor, can be similarly estimated by computing the neutron flight time from birth to disappearance by absorption or spatial leakage (Spriggs et al., 1997; Zoia et al., 2014a).

Extending the capabilities of Monte Carlo codes to adjoint-weighted kinetics parameters demands the adjoint flux $\varphi^\dagger$, which in principle requires the simulation of particles flowing backward from death to birth: in continuous-energy transport codes, this turns out to be a daunting task that is still a subject of active research (Hoogenboom, 2003). To overcome this obstacle, two strategies have been proposed so far: either resorting to perturbative techniques (Verboomen et al., 2006; Nagaya and Mori, 2010), or finding an estimate of $\varphi^\dagger$ that can be computed during forward simulations. For this latter, the early attempts based on the so-called Next Fission Probability (NFP) approximation for $\varphi^\dagger$ (Nauchi and Kameyama, 2005; Meulekamp and van der Marck, 2006) have been shown to be possibly flawed for large and/or strongly heterogeneous reactors (Nagaya et al., 2010; Nauchi and Kameyama, 2010). A major breakthrough has been nonetheless made possible by the rediscovery (Feghni et al., 2007, 2008; Nauchi and Kameyama, 2010; Kiedrowski, 2011b) of the so-called Iterated Fission Probability (IFP) interpretation of the adjoint flux $\varphi^\dagger$, originally formulated at the beginning of the nuclear era (Ussachoff, 1955; Weinberg, 1952; Hurwitz, 1964; Soodak, 1949). As detailed in the following, IFP enables the exact calculation of adjoint-weighted quantities, thus establishing Monte Carlo simulation as a reference tool for the analysis of kinetics parameters (Nauchi and Kameyama, 2010; Kiedrowski, 2011b; Shim et al., 2011). A number of production codes have integrated or are planning to integrate IFP capabilities: a non-exhaustive list includes MCNP5 (Kiedrowski, 2011a), SCALE (Perfetti, 2012), and SERPENT2 (Leppanen, 2014).

In this paper, we detail the implementation of the IFP method in TRIPOLI-4 [®], the reference Monte Carlo code developed at CEA (Brun et al., 2014; TRIPOLI-4 Project Team, 2012), for the calculation of Λ_{eff} and β_{eff} in view of a future release [1]. We will first illustrate the details of the adopted algorithm in Sec. 2, and then verify and validate the method on several reactor configurations in Sec. 3. We will finally discuss the impact of nuclear data libraries, cycle length and inter-cycle correlations on IFP in Sec. 4. Conclusions will be drawn in Sec. 5.

2. IFP and adjoint-weighted kinetics parameters

We will briefly recall the connection between the IFP method and the adjoint flux $\varphi^\dagger$, for the sake of completeness. Let us define $I(\vec{r}, E, \vec{\Omega})$ as the average number of descendant neutrons asymptotically produced in a distant generation g by a single neutron injected into the system with phase space coordinates $(\vec{r}, E, \vec{\Omega})$ at the initial time (in other words, I represents the
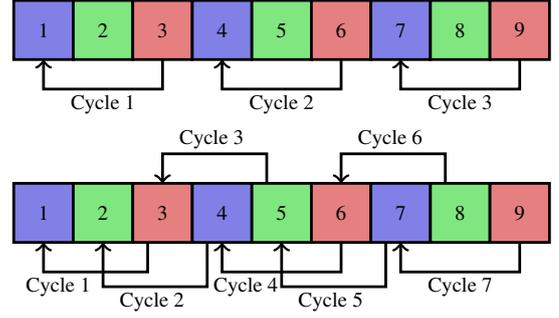
Figure 1: Top. IFP scheme with non-overlapping cycles. Bottom. IFP scheme with overlapping cycles. The arrows denote the link between the generation at which the scores are computed and the generation where the asymptotic neutron importance is estimated.

asymptotic importance of the injected neutron). By following the definition of I, it is possible to establish an exact balance equation (Nauchi and Kameyama, 2010; Ussachoff, 1955). Consider a small neutron path $d\vec{s} = \vec{r} - \vec{r}'' = \vec{\Omega}ds$: then, along $d\vec{s}$ we have

$$I(\vec{r}, E, \vec{\Omega}) = p_{nc} I(\vec{r} + \vec{\Omega}ds, E, \vec{\Omega}) + Q(\vec{r} + \vec{\Omega}ds, E, \vec{\Omega}), \quad (6)$$

where $p_{nc} = 1 - \Sigma_t ds$ is the non-collision probability, Σ_t being the total cross section, and Q is the average number of descendants for neutrons having a collision in $d\vec{s}$. Denote now by $q(\vec{r} + \vec{\Omega}ds, E \rightarrow E', \vec{\Omega} \rightarrow \vec{\Omega}')$ the average number of neutrons undergoing a collision during the flight ds and entering the phase space element $\vec{\Omega}', E'$, namely,

$$
\begin{aligned}
&q(\vec{r} + \vec{\Omega}ds, E \rightarrow E', \vec{\Omega} \rightarrow \vec{\Omega}') \\
&= \Sigma_s(\vec{r} + \vec{\Omega}ds, E \rightarrow E', \vec{\Omega} \rightarrow \vec{\Omega}')ds \\
&+ \frac{1}{k_{eff}} \frac{\chi_t(E \rightarrow E')}{4\pi} \nu_t \Sigma_f(\vec{r} + \vec{\Omega}ds, E)ds,
\end{aligned} \quad (7)
$$

where Σ_s is the scattering kernel, Σ_f is the fission cross section, ν_t is the average number of fission neutrons, and χ_t is the fission spectrum. The term Q can be then expressed as

$$
\begin{aligned}
&Q(\vec{r}, E, \vec{\Omega}) = \\
&\int_0^\infty dE' \int_0^{4\pi} d\Omega' q(\vec{r}, E \rightarrow E', \vec{\Omega} \rightarrow \vec{\Omega}') I(\vec{r}, E', \vec{\Omega}').
\end{aligned} \quad (8)
$$

Dividing (6) by ds and taking $ds \rightarrow 0$ we obtain

$$0 = \frac{dI(\vec{r}, E, \vec{\Omega})}{ds} - \Sigma_t I(\vec{r}, E, \vec{\Omega}) + \frac{Q(\vec{r} + \vec{\Omega}ds, E, \vec{\Omega})}{ds} \quad (9)$$

By developing the total derivative along $d\vec{s}$, Eq. (9) can be rewritten as

$$
\begin{aligned}
0 = &\Omega \cdot \nabla I(\vec{r}, E, \vec{\Omega}) - \Sigma_t I(\vec{r}, E, \vec{\Omega}) \\
&+ \int_0^\infty dE' \int_0^{4\pi} d\Omega' \Sigma_s(\vec{r}, E \rightarrow E', \vec{\Omega} \rightarrow \vec{\Omega}') I(\vec{r}, E', \vec{\Omega}') \\
&+ \frac{\nu_t \Sigma_f(\vec{r}, E)}{4\pi k_{eff}} \int_0^\infty dE' \int_0^{4\pi} d\Omega' \chi_t(E \rightarrow E') I(\vec{r}, E', \vec{\Omega}'). \quad (10)
\end{aligned}
$$

2

By inspection, the quantity $I(\vec{r}, E, \vec{\Omega})$ satisfies the adjoint Boltzmann equation for $\varphi^\dagger$, which implies that $I(\vec{r}, E, \vec{\Omega}) \propto \varphi^\dagger(\vec{r}, E, \vec{\Omega})$ (Nauchi and Kameyama, 2010; Ussachoff, 1955). This offers a practical means of estimating $\varphi^\dagger(\vec{r}, E, \vec{\Omega})$ by Monte Carlo methods: the adjoint neutron flux due to a neutron born at phase space coordinates $\vec{r}, E, \vec{\Omega}$ at a given generation g is proportional to the number of descendants of such neutron that will be found in the system at an asymptotic generation $g + M$, when M is sufficiently large (Nauchi and Kameyama, 2010). This provides the theoretical basis of the IFP method. As a particular case, choosing $M = 0$ leads to the the NFP approximation for $\varphi^\dagger$ (Nauchi and Kameyama, 2010).

2.1. The IFP algorithm

The IFP principles recalled above can be practically integrated in production Monte Carlo codes so as to estimate general adjoint-weighted scores (Nauchi and Kameyama, 2010; Kiedrowski, 2011b; Shim et al., 2011; Kiedrowski, 2011a; Perfetti, 2012; Leppanen, 2014), including sensitivity profiles based on first-order perturbations (Kiedrowski, 2011b) and exact perturbations (Truchet, 2014a,b). Here we will exclusively focus on the calculation of kinetics parameters, namely, the effective mean generation time Λ_{eff}, the effective delayed neutron fraction β_{eff} and the so-called Rossi alpha

$$\alpha_{\text{Rossi}} = -\frac{\beta_{\text{eff}}}{\Lambda_{\text{eff}}} = -\frac{\langle \varphi^\dagger, B\varphi \rangle}{\langle \varphi^\dagger, \frac{1}{v}\varphi \rangle}, \quad (11)$$

which is a key quantity occurring in reactivity measurements (Pfeiffer et al., 1974; Persson et al., 2008; Hansen, 1985; Cao and Lee, 2008; Bell and Glasstone, 1970; Keepin, 1965). The dot products involved in the definitions of effective kinetics parameters (Eqs. (4) and (11)) are evaluated by computing 1) the score associated to each fission neutron during the regular forward random walk of the particle at each generation g, and 2) the associated importance at a later generation $g + M$ by the IFP method. A unique identifier i is attributed to each fission neutron at generation g: this identifier will be transferred to all the descendants of the original particle (if any) along the following M so-called latent generations. The span from g to $g + M$ takes the name of IFP cycle, M being the cycle length. Memory is also kept of whether or not this neutron was issued from a prompt or a delayed fission. During generation $g + M$, fission neutrons originating from the original ancestor with identifier i (if any) are recorded, and allow thus estimating the asymptotic importance. In particular, the importance is denoted $(\text{ifp}_p)_i$ if the ancestor neutron was issued from a prompt fission, and $(\text{ifp}_d)_i$ if the ancestor neutron was issued from a delayed fission. The adjoint-weighted delayed fission score associated to an history can be expressed as

$$\frac{1}{k_{\text{eff}}}\langle \varphi^\dagger, B\varphi \rangle_{\text{history}} = \varphi^\dagger_{d1}w_{d1} + \varphi^\dagger_{d2}w_{d2} + ...$$
$$= \sum_i \varphi^\dagger_{di}w_{di} = \sum_i \frac{(\text{ifp}_d)_i}{w_{di}}w_{di} = \sum_i (\text{ifp}_d)_i. \quad (12)$$

In Eq. (12), the delayed neutron simulation weight w_{di} of each collision i cancels when being multiplied by the related delayed neutron adjoint flux $\varphi^\dagger_{di}$. The adjoint-weighted total fission score for the same history can be similarly evaluated as the sum of prompt and delayed contributions, namely,

$$\frac{1}{k_{\text{eff}}}\langle \varphi^\dagger, P\varphi \rangle_{\text{history}} = \sum_i (\text{ifp}_p)_i + \sum_i (\text{ifp}_d)_i = \sum_i (\text{ifp})_i. \quad (13)$$

When averaging over all contributions coming from the ensemble of simulated neutron histories, Eq. (12) converges to $\langle \varphi^\dagger, B\varphi \rangle / k_{\text{eff}}$ and Eq. (13) to $\langle \varphi^\dagger, P\varphi \rangle / k_{\text{eff}}$, respectively. Then, the ratio of (12) over (13) yields β_{eff}. Finally, the adjoint-weighted total neutron lifetime can be estimated as

$$\langle \varphi^\dagger, \frac{1}{v}\varphi \rangle_{\text{history}} = \sum_i [(\text{ifp}_p)_i + (\text{ifp}_d)_i]t_i, \quad (14)$$

where t_i is the neutron lifetime at collision i, counted from its birth in generation g.

The central issue of the IFP algorithm is the tracking of the neutron identifier from generation g to generation $g + M$. In Tripoli-4 ® we have decided to start a new IFP cycle at each generation g, which gives rise to an overlapping structure of superposed IFP cycles (each having the same length M), as illustrated in Fig. 1 (bottom). A similar approach has been recently proposed for the Monte Carlo code SERPENT (Leppanen, 2014) and shown to yield no significant increase in computer memory requirements with respect to the sequential non-overlapping IFP scheme originally proposed in (Kiedrowski, 2011a) and displayed in Fig. 1 (top). Each fission neutron that begins a new history is attributed a unique identifier that belongs to the current generation g. Just before the assignment, an array keeps record of the former neutron identifier that had been assigned in the previous generation. At each subsequent generation, a new array of this type is created and the previous is deleted. It is then possible to track the identifiers from generation to generation, up to a maximum number specified by the user. Starting a new IFP cycle at each generation improves the statistics of kinetics parameters by a factor $\sqrt{M}$ (for fixed number of total generations in the criticality calculation), but it also increases inter-cycle correlations. This issue will be briefly addressed in Sec. 4.

3. Verification and validation tests

In this Section we present extensive verification and validation tests for the IFP algorithm described above.

3.1. Infinite system with two energy groups

As a first verification test, we address an homogeneous system of infinite size, with two energy groups v_1 (rapid) and v_2 (thermal) and two delayed families a and b. Assuming, as in (Kiedrowski, 2010), that there is no up-scattering, that prompt neutrons are emitted in group $g = 1$ alone, and that fissions can be induced only from neutrons colliding in group

3
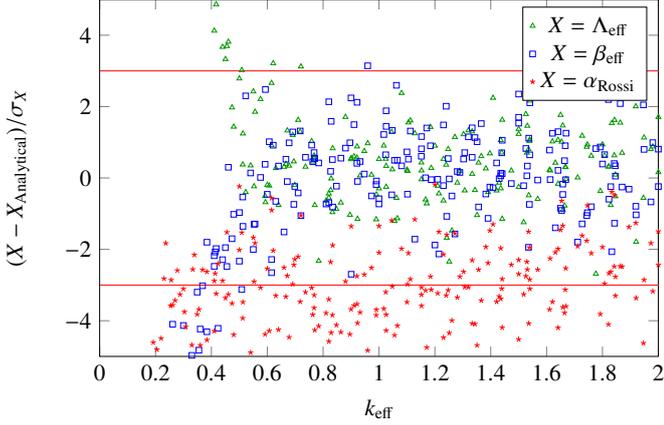
Figure 2: Discrepancies between calculated and analytical values of Λ_{eff}, β_{eff} and α_{Rossi} (normalized to respective standard deviations σ). Monte Carlo simulations have been performed with 2000 neutrons per generation and 2700 active IFP cycles. Each point identifies a reactor configuration where the parameters $\nu_{f,2}$ and $\Sigma_{a,g}$ have been modified around their reference values. The corresponding k_{eff} value for each configuration is used in abscissas.

Figure 3: Discrepancies between calculated and analytical values of Λ_{eff}, β_{eff} and α_{Rossi} (normalized to respective standard deviations σ). Monte Carlo simulations have been performed with 10000 neutrons per generation and 2700 active IFP cycles. Each point identifies a reactor configuration where the parameters $\nu_{f,2}$ and $\Sigma_{a,g}$ have been modified around their reference values. The corresponding k_{eff} value for each configuration is used in abscissas.

$g = 2$, yields the following system of equations for the scalar flux φ

$$\Sigma_{r,1}\varphi_1 = \frac{1}{k_{\text{eff}}}(1 - \beta_{\text{tot}} + \xi_1)\nu_{f,2}\Sigma_{f,2}\varphi_2$$

$$\Sigma_{r,2}\varphi_2 = \Sigma_{s,12}\varphi_1 + \frac{1}{k_{\text{eff}}}\xi_2\nu_{f,2}\Sigma_{f,2}\varphi_2, \tag{15}$$

where we have set $\varphi_g = \varphi(v_g)$ and $\Sigma_{x,g} = \Sigma_x(v_g)$. Here $\Sigma_{s,gj} = \Sigma_s(v_g \rightarrow v_j)$ is the differential scattering kernel, $\Sigma_{r,g} = \Sigma_{t,g} - \Sigma_{s,gg}$ the removal cross-section of group g, $\Sigma_{f,g}$ the fission cross-section of group g, $\nu_{f,g}$ the number of neutrons produced by a fission in group g, $\chi_{i,g}$ is the delayed neutron spectrum from delayed family i to energy group g, β_i the delayed neutron fraction of family i, $\beta_{\text{tot}} = \beta_a + \beta_b$, and $\xi_g = \chi_{a,g}\beta_a + \chi_{b,g}\beta_b$. For this simple configuration, the explicit solutions for the forward and adjoint fluxes can be obtained by algebraic manipulations. Hence, the kinetics parameters β_{eff}, Λ_{eff} and α_{Rossi} can be computed analytically as a function of the physical parameters, as described in (Kiedrowski, 2010). More precisely, we obtain

$$\beta_{\text{eff}} = \frac{\frac{\Sigma_{s,12}}{\Sigma_{r,1}}\xi_1 + \xi_2}{\frac{\Sigma_{s,12}}{\Sigma_{r,1}}(1 - \beta_{\text{tot}} + \xi_1) + \xi_2},$$

$$\Lambda_{\text{eff}} = \frac{\frac{1}{v_1}\frac{\Sigma_{s,12}}{\Sigma_{r,2}} + \frac{1}{v_2}\frac{\Sigma_{s,12}}{\Sigma_{r,2}-\xi_2\nu_{f,2}\Sigma_{f,2}}}{\left(\frac{\Sigma_{s,12}}{\Sigma_{r,1}}(1 - \beta_{\text{tot}} + \xi_1) + \xi_2\right)\frac{\nu_{f,2}\Sigma_{f,2}\Sigma_{s,12}}{\Sigma_{r,2}-\xi_2\nu_{f,2}\Sigma_{f,2}}}, \tag{16}$$

whence also

$$\alpha_{\text{Rossi}} = -\frac{(\frac{\Sigma_{s,12}}{\Sigma_{r,1}}\xi_1 + \xi_2)\frac{\nu_{f,2}\Sigma_{f,2}\Sigma_{s,12}}{\Sigma_{r,2}-\xi_2\nu_{f,2}\Sigma_{f,2}}}{\frac{1}{v_1}\frac{\Sigma_{s,12}}{\Sigma_{r,2}} + \frac{1}{v_2}\frac{\Sigma_{s,12}}{\Sigma_{r,2}-\xi_2\nu_{f,2}\Sigma_{f,2}}}. \tag{17}$$

These expressions provide a reliable verification benchmark for the IFP algorithm. To this aim, the continuous-energy code TRIPOLI-4 ® has been modified so as to handle multi-group

transport. As a reference configuration, we have chosen the values of the parameters as in Tab. 1, with $\beta_a = 1/4$, $\beta_b = 1/8$, $v_1 = 1$ and $v_2 = 1/2$, which yields an exactly critical system. Then, the number of neutrons per fission $\nu_{f,2}$ and the absorption cross section $\Sigma_{a,g}$ have been modified around their reference values and the corresponding kinetics parameters have been computed by Monte Carlo simulation and compared to the exact solutions. The outcomes of these simulations are displayed in Fig. 2 as a function of the resulting effective multiplication factor k_{eff}. In order to assess the convergence of the IFP algorithm to the exact values in Eqs. (16) and (17), we display the ratio $(X - X_{\text{Analytical}})/\sigma_X$, where X is β_{eff}, Λ_{eff} or α_{Rossi}, and σ_X is the statistical uncertainty of the Monte Carlo calculation.

Since the medium is homogeneous and the energy dependence is weak (only two speeds), the convergence of the IFP algorithm is rather fast, and several tests allow concluding that $M = 5$ latent generations are sufficient to attain the asymptotic convergence for this simple example. A good agreement between the Monte Carlo results and the reference analytical values is found for both Λ_{eff} and β_{eff} for reactor configurations in the region $k_{\text{eff}} > 0.5$ (see Fig. 2). For reactor configurations pertaining to the region $k_{\text{eff}} < 0.5$ the convergence of the power iteration in the criticality simulation is rather poor, and numerical results are affected by a large statistical uncertainty. The convergence of α_{Rossi} appears to be affected by a slight bias with respect to the exact solution, which progressively vanishes by increasing the number of simulated neutrons per generation, as shown in Fig. 3. This behavior is due to the

g	Σ_{rg}	ν_{fg}	Σ_{fg}	$\chi_{a \rightarrow g}$	$\chi_{b \rightarrow g}$	$\Sigma_{s,g \rightarrow 1}$	$\Sigma_{s,g \rightarrow 2}$	$\Sigma_{\text{tot}g}$
1	1.5	0	0	3/4	1/2	1/2	1/2	2
2	2	24/5	1	1/4	1/2	0	1	3

Table 1: Reference physical parameters adopted in the verification models.

fact that the Monte Carlo code for practical reasons computes the kinetics parameters in Eqs. (4) and (11) as averages of ratios of fluctuating quantities, instead of ratios of averages of fluctuating quantities: this introduces a systematic bias, whose relevance is expected to decrease as the number of particles per generation increases. Not surprisingly, the statistical bias becomes particularly evident for α_{Rossi}, which is the ratio of the two most fluctuating quantities, namely, the delayed productions $\langle \varphi^\dagger, B\varphi \rangle$ and the lifetime $\langle \varphi^\dagger, \frac{1}{v}\varphi \rangle$. As a matter of fact, it would be possible to obtain α_{Rossi} as a ratio of the statistical series, measured at each generation. The uncertainty would be then provided by the standard deviation of the ratio of a sum, in the form $\sigma(\sum_i X_i / \sum_i Y_i)$, which can be calculated by using bootstrapping or jackknife methods.

3.2. The rod model with two energy groups

The rod model is possibly the simplest example of space- and direction-dependent transport problem (Montagnini and Pierpaoli, 1971): particles move along a line (the rod) and undergo collision events at a rate $v_g\Sigma_{t,g}$. Because of the geometric constraints, only two directions of flight are allowed, namely forward ($\mathbf{\Omega} = +$) and backward ($\mathbf{\Omega} = -$); here, we furthermore assume that scattering and fission are isotropic, i.e., directions taken by the particles after a collision are sampled with equal probability, a single fissile isotope is present, there is no up-scattering, prompt neutrons are emitted in group $g = 1$ alone, and fissions can be induced only from neutrons colliding in group $g = 2$. If we define $\varphi(x, +)$ the angular flux in the positive direction and $\varphi(x, -)$ in the negative direction, respectively, where x is the spatial coordinate, the transport equations for two energy groups become

$$\pm \frac{\partial \varphi_1}{\partial x}(x, \pm) + \Sigma_{t,1}\varphi_1(x, \pm) =$$

$$\Sigma_{s,11}\varphi_1(x) + \frac{1}{k_{\mathrm{eff}}}(1 - \beta_{\mathrm{tot}} + \xi_1)v_{f,2}\Sigma_{f2}\varphi_2(x), \quad (18)$$

$$\pm \frac{\partial \varphi_2}{\partial x}(x, \pm) + \Sigma_{t,2}\varphi_2(x, \pm) =$$

$$\Sigma_{s,22}\varphi_2(x) + \Sigma_{s,12}\varphi_1(x) + \frac{1}{k_{\mathrm{eff}}}\xi_2 v_{f2}\Sigma_{f,2}\varphi_2(x), \quad (19)$$

where $\varphi_g(x) = [\varphi_g(x, +) + \varphi_g(x, -)]/2$ is the scalar flux integrated over the allowed directions. Explicit solutions for the kinetics parameters of the rod model can be obtained in principle, but the calculations are quite cumbersome. Instead, we have computed β_{eff}, Λ_{eff} and α_{Rossi} numerically by direct integration of the transport equations and the associated adjoint equations. Results for this example are illustrated in Fig. 4 for the physical parameters given in Tab. 1. The size L of the rod is varied in the interval $1 < L < 10$, and we compare the reference values to the outcomes of the Monte Carlo simulations. Each reactor configuration is identified by the corresponding value of k_{eff}. Similarly as in the previous example, the IFP algorithm converges to the reference values.

3.3. The Rossi alpha validation suite

The parameter α_{Rossi} can be directly measured in low-power reactor configurations close to delayed criticality by resorting
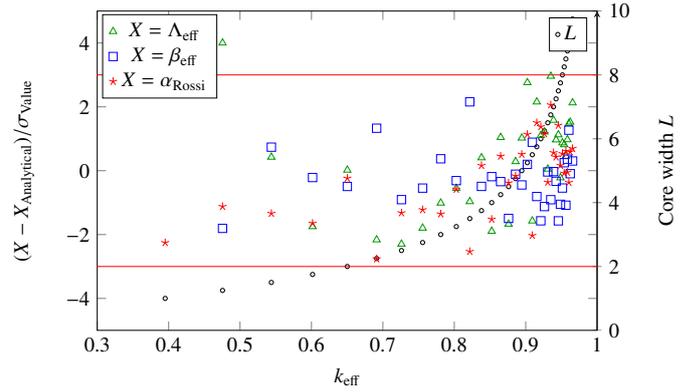
Figure 4: Discrepancies between calculated and analytical values of Λ_{eff}, β_{eff} and α_{Rossi} (normalized to respective standard deviations σ). Monte Carlo simulations have been performed with 10000 neutrons per generation and 2700 active IFP cycles. Each point identifies a reactor configuration where the rod length L has been modified in $1 < L < 10$. The corresponding k_{eff} value for each configuration is used in abscissas.

to neutron noise analysis techniques (Hansen, 1985; Keepin, 1965; Bell and Glasstone, 1970). When available, these measurements thus provide an invaluable means of validating the IFP algorithm. As a first test, we consider the Rossi alpha validation suite (Kiedrowski et al., 2011), which contains a collection of experimental measurements of α_{Rossi} for a series of reactor mock-up configurations together with the corresponding benchmark specifications from (OECD NEA, 2010). The Monte Carlo calculations results obtained with the IFP method implemented in MCNP are also reported in the same document (Kiedrowski et al., 2011). For our simulations, we have chosen the ENDF/B-VII.0 nuclear data library in order to be consistent with the choice of (Kiedrowski et al., 2011). The number of neutrons per generations is 40000, and the IFP cycle length is $M = 20$. The results obtained with TRIPOLI-4® are resumed in Tab. 3, where they are compared to the experimental measurements and to those obtained with MCNP by using the same nuclear data library (as reported in (Kiedrowski et al., 2011)). For all tested configurations, the values computed by TRIPOLI-4® are in good agreement with the experimental measurements. Where slight discrepancies are observed, the α_{Rossi} computed by TRIPOLI-4® is in agreement with the value computed by MCNP: as pointed out in (Kiedrowski et al., 2011), the experimental uncertainty reported in the Rossi alpha suite does not include physical uncertainties, so that part of the discrepancies between Monte Carlo simulations and experimental data could be attributed to such factors as physical dimensions and material densities. Moreover, slight inaccuracies in a few isotopes of the nuclear data library (for instance ^{233}U and the unresolved resonance range of ^{235}U (Kiedrowski et al., 2011)) might play a role for some of the configurations. In all configurations, the statistical bias on the α_{Rossi} estimator is small, thanks to the large number of neutrons per generation. For reference, in Fig. 5 we display the statistical bias $-(\alpha_{\mathrm{Rossi}} + \beta_{\mathrm{eff}}/\Lambda_{\mathrm{eff}})/(\beta_{\mathrm{eff}}/\Lambda_{\mathrm{eff}})$ for the GODIVA configuration as a function of the number of particles per generation: for this ex-

ample, the bias becomes negligible above 5000 simulated particles per generation.

For some of the reactor configurations of the Rossi alpha validation suite, experimental values of β_{eff} are also available (Paxton, 1981). The comparison between the measured β_{eff} and the results of Tʀɪᴘᴏʟɪ-4 ® and MCNP by resorting to ENDF/B-VII.0 nuclear data library are shown in Tab. 4. For reference, in the same table we also display the values of β_{eff} computed with Tʀɪᴘᴏʟɪ-4 ® by using the NFP method and the average delayed neutron fraction β_0. As expected on physical grounds, the results obtained by resorting to the IFP with a large M are in better agreement with experimental data as compared to un-weighted kinetics parameters. The NFP is in fairly good agreement with IFP in most cases, except for reflected configurations (such as FLATTOP), where large deviations are observed: in these cases, space and energy effects become important, and choosing $M = 0$ yields a poor approximation of the adjoint flux (Nagaya et al., 2010; Nauchi and Kameyama, 2010). The un-weighted parameter β_0 typically shows large differences with respect to the IFP β_{eff}.

Once the kinetics parameters α_{Rossi} and β_{eff} have been determined experimentally, the value of the mean neutron generation time Λ_{eff} can be consistently computed as $\Lambda_{\mathrm{eff}} = -\beta_{\mathrm{eff}}/\alpha_{\mathrm{Rossi}}$ (Paxton, 1981). To complete our analysis, the values of Λ_{eff} are displayed in Tab. 5. The results obtained by Tʀɪᴘᴏʟɪ-4 ® by resorting to ENDF/B-VII.0 nuclear data library are in good agreement with the calculated Λ_{eff} and with those obtained by MCNP. For comparison, we also display the values of Λ_{eff} computed with Tʀɪᴘᴏʟɪ-4 ® by using the NFP method and the un-weighted average neutron generation time Λ_0. Similarly as in the case of β_{eff}, the results obtained by resorting to the IFP with a large M are in better agreement with experimental data as compared to un-weighted kinetics parameters. For reflected configurations, large deviations are again observed between NFP and IFP. The un-weighted parameter Λ_0 typically shows large differences with respect to the IFP Λ_{eff}: to support our analysis, we finally display the values of Λ_0 computed by MCNP [2], which are in excellent agreement with those computed by Tʀɪᴘᴏʟɪ-4 ®.

3.4. The CALIBAN reactor facility at CEA/Valduc

The CALIBAN reactor is a super prompt critical configuration operated by CEA/Valduc that is used for criticality analysis. The detailed reactor description and the corresponding experimental measurements of the α_{Rossi} parameter are given in (Richard, 2013). We have performed Monte Carlo calculations for CALIBAN by using the JEFF3.1.1 nuclear data library with 40000 particles per generation and $M = 20$. The value of α_{Rossi} estimated by Tʀɪᴘᴏʟɪ-4 ®, $\alpha_{\mathrm{Rossi}} = -65.8 \pm 0.8$ s^{-1}, is in good agreement with the experimental measurements, $\alpha_{\mathrm{Rossi}} = -64 \pm 1$ s^{-1}, reported in (Richard, 2013).
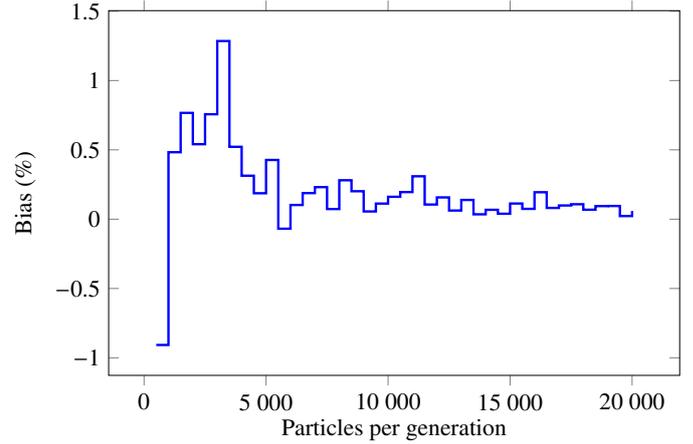
Figure 5: The GODIVA configuration of the Rossi alpha validation suite. The statistical bias on the α_{Rossi} estimator as a function of the number of simulated neutrons per generation.

3.5. The MISTRAL reactor facility at CEA/Cadarache

The MISTRAL facility is operated at CEA/Cadarache: MISTRAL1 has an enriched UO_2 (3.7 % of ^{235}U) core with about 750 PWR-type fuel pins; MISTRAL2 has 100 % MOX (7 % Pu) core with about 1600 fuel pins arranged in the same lattice pitch as MISTRAL1. The detailed description of the cores and the corresponding experimental measurements of the β_{eff} parameter are available in (Santamarina et al., 2012). We have performed Monte Carlo calculations for MISTRAL1 and MISTRAL2 by using the JEFF3.1.1 nuclear data library with 40000 particles per generation and $M = 20$. The values of β_{eff} estimated by Tʀɪᴘᴏʟɪ-4 ® are coherent with the experimental values reported in (Santamarina et al., 2012) (see Tab. 6). For comparison, the results obtained by using the APOLLO-2 deterministic SHEM-MOC calculation scheme (Santamarina et al., 2013) are also collected in the same table.

3.6. The ORPHEE reactor facility at CEA/Saclay

The ORPHEE facility is located at CEA/Saclay and jointly operated by CEA and CNRS [3]. ORPHEE is a pool-type research reactor whose main goal is to produce neutron beams for neutron scattering experiments with a broad wavelength and energy distribution. The core of ORPHEE is very small in size and highly enriched in ^{235}U, providing a high neutron density, with a heavy water reflector tank. A detailed description of the facility and the related α_{Rossi} measurements performed during the initial rod worth calibration campaign are reported in the nuclear safety report (Rapport de Sûreté, 1981). The measurements yield $\alpha_{\mathrm{Rossi}} \simeq -40$ s^{-1} (the experimental uncertainty was unfortunately not reported in (Rapport de Sûreté, 1981)). Calculations performed with Tʀɪᴘᴏʟɪ-4 ® by using JEFF3.1.1 nuclear data library, with 10^4 particles per generation and $M = 20$, give $\alpha_{\mathrm{Rossi}} = -41.1 \pm 0.3$ s^{-1} (Zoia et al., 2014b), which is

---

[2]Actually, the code MCNP computes the un-weighted neutron removal time T_0 (X-5 Monte Carlo Team, 2003), from which $\Lambda_0 = T_0/k_{\mathrm{eff}}$ can be easily deduced.

[3]Laboratoire Léon Brillouin. See the website: http://www-llb.cea.fr/

in good agreement with the experimental data. As for the delayed neutron fraction, the measurement quoted in the nuclear safety report is β_{eff} = 744 pcm (Rapport de Sûreté, 1981), to be compared with the value β_{eff} = 747.8 ± 3.9 pcm computed by TRIPOLI-4 [®] (Zoia et al., 2014b).

4. Discussion

4.1. Sensitivity to nuclear data library

The calculations of the IFP kinetics parameters in the previous Section have been performed by selecting a specific nuclear data library, either `ENDF/B-VII.0` or `JEFF3.1.1`. In order to evaluate the impact of the nuclear data on the obtained results, we have re-run some of the configurations of the Rossi alpha validation suite by resorting to the `JEFF3.1.1` library. The comparison with respect to `ENDF/B-VII.0` for the α_{Rossi} parameter is reported in Tab. 7. In most cases, the discrepancies on the α_{Rossi} parameter are rather weak, and lie within a few percent. In order to single out the distinct contributions to the observed discrepancies, the cases of β_{eff} and Λ_{eff} are separately shown in Tabs. 8 and 9, respectively.

4.2. Choosing the IFP cycle length

The length M of the IFP cycle is an important parameter to be chosen before running the simulation. Typically, one assumes that $M \simeq 10$ up to $M \simeq 20$ latent generations are sufficient for the descendant neutrons to converge to the asymptotic adjoint flux. The value of M is of course problem-dependent: configurations where spectral and/or geometrical effects play a relevant role will generally speaking require a larger value of M to reach the asymptotic convergence of the adjoint flux. In TRIPOLI-4 [®], we have implemented a diagnostic tool that allows the convergence of the IFP method to be displayed as a function of M. This tool benefits from the structure of superposed cycles so as to process the results of the IFP algorithm for different cycle lengths 1, 2, $\cdots$, up to the maximum value M required by the user. An example of such analysis is illustrated in Fig. 6 (top) for the GODIVA configuration from the Rossi alpha validation suite. For this case, we have chosen the rather extreme value $M = 100$ and we have separately computed β_{eff} and Λ_{eff} as a function of the IFP cycle length M. It is immediately apparent that after approximately 10 latent generations the kinetics parameters converge to their respective asymptotic values. At the same time, the statistics of β_{eff} and Λ_{eff} deteriorates for growing M (for a fixed number of simulated particles), as expected on physical grounds: for very large M, the number of descendant neutrons that are still associated to the identifier of the first generation g might be considerably reduced, since at each generation there exists a finite probability that the current fission chain comes to an end. The same convergence analysis has been performed also on a full PWR reactor core of type N4, representative of the French 1450 MW PWR fleet (Leconte, 2010). Results for the delayed neutron fraction β_{eff} and the mean generation time Λ_{eff} are displayed in Fig. 6 (bottom). The convergence pattern is quite similar to that obtained for GODIVA, in spite of the conspicuous difference in size of the two systems.
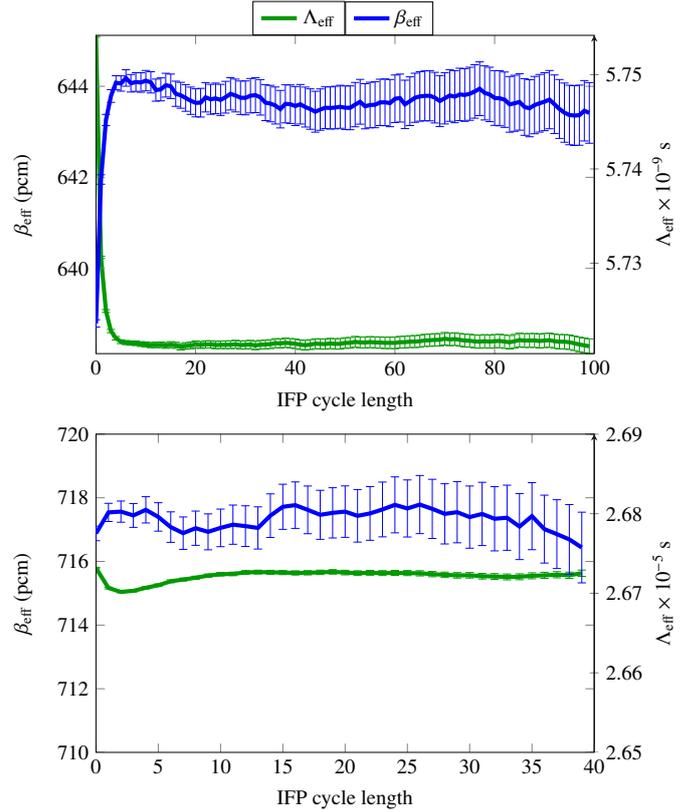
Figure 6: Top. The kinetics parameters β_{eff} and Λ_{eff} as a function of the IFP cycle length M for the GODIVA configuration of the Rossi alpha validation suite. Error bars represent statistical uncertainty at 1σ. Bottom. The kinetics parameters β_{eff} and Λ_{eff} as a function of the IFP cycle length M for the N4 PWR reactor. Error bars represent statistical uncertainty at 1σ.

In principle, it would be possible to establish some selection criteria for an optimum value of M. For instance, one might identify the optimum cycle length as the smallest value of M whose associated statistics for the kinetics parameters is compatible within 1σ uncertainty with the values obtained for longer cycles. The results corresponding to the application of these criteria are resumed in Tab. 2 for some of the reactor configurations described above. In most cases, it is apparent that the selection criteria are (not surprisingly) strongly problem-dependent.

4.3. Inter-cycle correlations

The power iteration algorithm is intrinsically based on the idea of sampling the source of the fission neutrons for the next generation on the basis of the fission sites determined during the current generation. This in turn induces correlations between (local as well as global) scores computed by averaging the statistics over several generations (which are assumed to be stationary realizations of the same stochastic process). Fluctuations around average values appear because of Monte Carlo simulations being intrinsically based on the transport of a finite number of particles: by increasing the number of simulated histories, it is well known that the fluctuations affecting the

Configuration	β_{eff}	Λ_{eff}	α_{Rossi}
JEZEBEL-233	1	4	2
FLATTOP-23	3	5	12
GODIVA	2	8	8
FLATTOP-25	5	4	8
STACY-30	1	6	3
STACY-46	2	10	6
JEZEBEL	2	5	3
FLATTOP-PU	3	5	4
THOR	0	4	3
N4 (Full size PWR)	1	9	2

Table 2: Optimal IFP cycle lengths M.

computed scores are progressively reduced (Lux and Koblinger, 1991; Brown, 2005). Another source of noise specific to Monte Carlo criticality calculations is related to fission events, because of two concurrent phenomena: *i*) fissions induce splitting of the trajectories, which increases the dispersion of the population number within a given volume; *ii*) the birth of a neutron occurring at a fission site induces correlations between particle positions (Lux and Koblinger, 1991; Sjenitzer and Hoogenboom, 2011; Dumonteil et al., 2014). As a consequence, the variance of the obtained Monte Carlo scores might be underestimated with respect to the ideal case of truly independent simulations. The kinetics parameters, which are computed by resorting to the power iteration, suffer from the same problem. Moreover, the fact of using superposed IFP cycles potentially increases the existing inter-generation correlations (nonetheless, the average value is not affected). In particular, we have

$$\sigma^2 = \text{var}(x_i) + 2\sum_k \text{cov}(x_i, x_{i+k}), \qquad (20)$$

where $\text{var}(x_i)$ is the usual variance estimated from a sample of n terms, namely,

$$\text{var}(x_i) = \frac{\sum_i^n (x_i - \overline{x})^2}{n} \qquad (21)$$

In order to investigate the impact of inter-cycle correlations on the variance of kinetics parameters, N independent Monte Carlo simulations have been performed using different random generator seeds. For each run $i \in N$, n realizations of the kinetics parameters have been sampled, so as to compute a mean x_i, a standard deviation σ_i and a standard error $\hat{\sigma}_i = \frac{\sigma_i}{\sqrt{n}}$, where the values σ_i are obtained by using Eq. (21). The effects of inter-cycle correlations are mirrored in $\hat{\sigma}_i$, which can be underestimated (if the realizations are correlated) or overestimated (if the realizations are anti-correlated). By construction, the computed $\hat{\sigma}_i$ are strictly independent, so that they can be combined in order to obtain a global value called the apparent standard error $\hat{\sigma}_a$, namely,

$$\hat{\sigma}_a = \frac{\sqrt{\sum_i \sigma_i^2 / N}}{\sqrt{Nn}} = \frac{\sqrt{\sum_i \sigma_i^2 / N}}{\sqrt{Nn}} = \frac{\sqrt{\sum_i \hat{\sigma}_i^2}}{N}. \qquad (22)$$

Since Monte Carlo runs are independent, the standard error can be rigorously estimated as

$$\hat{\sigma} = \frac{\sigma}{\sqrt{N}} = \frac{\sqrt{\sum_i^N (x_i - \overline{x})^2}}{N} \qquad (23)$$

Then, the impact of inter-cycle correlations can be roughly assessed by computing the ratio $f = \hat{\sigma}/\hat{\sigma}_a$ as in (Mervin et al., 2011). Several tests have been performed on a selection of the reactor configurations from the Rossi alpha validation suite presented above. For each configuration, $N = 1000$ independent runs were performed, with $n = 900$ active IFP cycles. The number of neutrons per generation is relatively small (500), in order to enhance the effects of correlations. In Fig. 7, the quantity f is plotted as a function of the IFP cycle length. For both β_{eff} and Λ_{eff}, f shows only slight deviations from unit, which means that the impact of inter-cycle correlations for the examples considered here is rather weak. The relevance of correlations increases for decreasing cycle length M: for small M, f rises up to $f \simeq 1.1$. The case of the N4 PWR has been also analyzed in Fig. 8, with $N = 100$ and $n = 900$. For this configuration, the correlations on β_{eff} are weak, whereas those on Λ_{eff} rise up to $f \simeq 1.6$ for low cycle length M: this is almost surely due to the large size of the $N4$ core, which possibly enhances intercycle correlations due to the distribution of fission source sites. Rather surprisingly, Λ_{eff} is only slightly affected by the number of particles per generation.

5. Conclusions

In this paper we have described the specific implementation of the IFP algorithm in the reference Monte Carlo code Tripoli-4 ® developed at CEA, with the aim of computing the adjoint-weighted kinetics parameters β_{eff} and Λ_{eff}. We have adopted a scheme based on superposed IFP cycles, which has shown good performances in terms of memory requirements and computational cost. The proposed algorithm has been first verified on several simplified reactor configurations where exact values of β_{eff} and Λ_{eff} were available: in all tested problems, a good agreement has been found between exact and computed kinetics parameters. Then, the IFP method implemented in Tripoli-4 ® has been validated on a selection of reactor configurations, including the Rossi alpha validation suite benchmarks and some experimental reactor mock-ups operated at CEA. The validation has concerned in particular β_{eff} and $\alpha_{\text{Rossi}} = -\beta_{\text{eff}}/\Lambda_{\text{eff}}$, which can be measured experimentally in nuclear reactors operated at low power or during startup. Results obtained by comparing the Tripoli-4 ® estimates to benchmark and/or experimental values have been satisfactory. Special attention has been paid to the impact of the nuclear data libraries on the Monte Carlo estimates. The choice of IFP cycle length and the relevance of inter-cycle correlations due to the use of a superposed-cycles scheme have been also examined in detail.
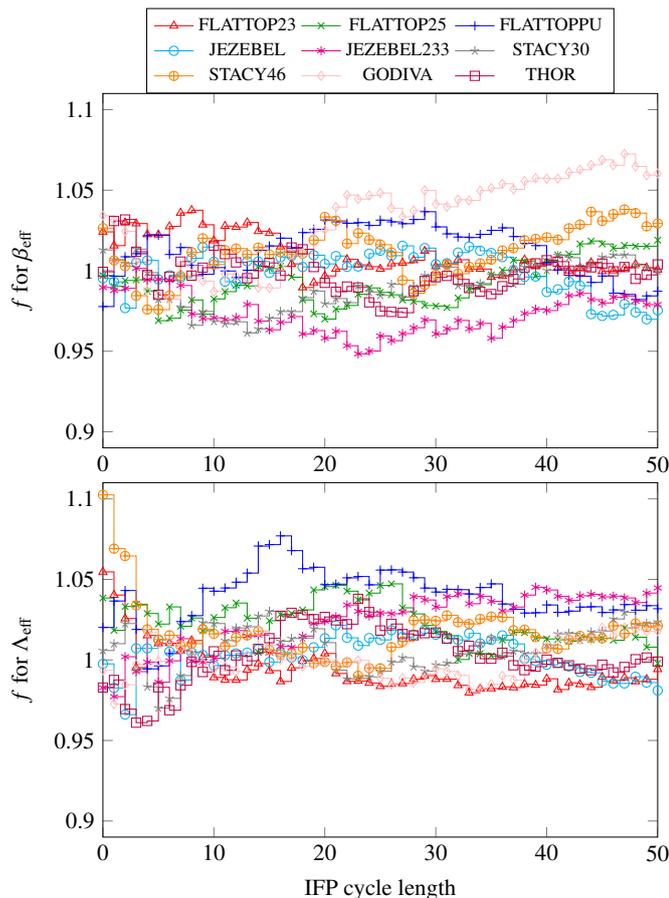
Figure 7: Inter-cycle correlations on β_{eff} and Λ_{eff} for some of the reactor configurations in the Rossi alpha validation suite. The factor $f = \hat{\sigma}/\hat{\sigma}_a$ is plotted as a function of the IFP cycle length M. Large deviations from $f \simeq 1$ imply strong inter-cycle correlations.

Figure 8: Inter-cycle correlations on β_{eff} and Λ_{eff} for the $N4$ PWR reactor. The factor $f = \hat{\sigma}/\hat{\sigma}_a$ is plotted as a function of the IFP cycle length M. Large deviations from $f \simeq 1$ imply strong inter-cycle correlations.

Acknowledgments

Albertoni, S., Montagnini, B., 1966. J. Math. Anal. and Appl. **13**, 19.

Bell, G. I., Glasstone, S., 1970. Nuclear reactor theory, Van Nostrand Reinhold Company.

Brown, F., 2005. LA-UR-05-4983, Los Alamos National Laboratory.

Brun, E., et al., 2014. Ann. Nucl. En. *In press.*

Cao, Y., Lee, J. C., 2008. Nucl. Sci. Eng. **165**, 270.

Cohen, E. R., 1958. In *Proceedings of the 2nd UN conference of the peaceful uses of atomic energy*, P/629, Geneva, Switzerland.

Dumonteil, E., Malvagi, F., Zoia, A., Mazzolo, A., Artusio, D., Dieudonné, C., De Mulatier, C. 2014. Ann. Nucl. En. **63**, 612.

Feghhi, S. A. H., Shahriari, M., Afarideh, H., 2007. Ann. Nucl. En. **34**, 514.

Feghhi, S. A. H., Shahriari, M., Afarideh, H., 2008. Ann. Nucl. En. **35**, 1397.

Hansen, G. E., 1985. LA-UR-85-4176.

Henry, A. F., 1958. Nucl. Sci. Eng. **3**, 52.

Hoogenboom, J. E., 2003. Nuc. Sci. Eng. **143**, 99.

Hurwitz Jr., H., 1964. In: Radkowsky, A. (Ed.), Naval Reactors Physics Handbook, vol. I. Naval Reactors, Division of Reactor Development, United States Atomic Energy Commission, pp. 864.

Keepin, G. R., 1965. Physics of Nuclear Kinetics, Addison-Wesley, Reading, UK.

Kiedrowski, B. C., 2010. LA-UR-10-01803, Los Alamos.

Kiedrowski, B. C., PhD thesis, 2011. Michigan University.

Kiedrowski, B. C., Brown, F. B., Wilson, P. P. H., 2011. Nucl. Sci. Eng. **68**, 226.

Kiedrowski, B. C., et al., 2011. LA-UR-11-04409, Los Alamos.

Kiedrowski, B. C., 2011. LA-UR-10-01700, Los Alamos.

Leconte, P., Vidal, J. F., Kerkar, N., 2010. In *Proceedings of the PHYSOR 2010 conference*, Pittsburgh, USA.

Leppänen, J., et al., 2014. ann. Nucl. Energy **65**, 272.

Lux, I., Koblinger, L., 1991. Monte Carlo particle transport methods: Neutron and photon calculations, CRC Press, Boca Raton.

Montagnini, B., Pierpaoli, V., 1971. Transp. Theory and Stat. Phys. **1**, 59.

Meulekamp, R. K., van der Marck, S. C., 2006. Nucl. Sci. Eng. **152**, 142.

Mervin, B. T., et al., 2011. In *Proceedings of the M&C 2011 Conference*, Rio de Janeiro, Brazil.

Nagaya, Y. et al., 2010. Ann. Nucl. En. **37**, 1308.

Nagaya, Y., Mori, T., 2011. Ann. Nucl. En. **38**, 254.

Nauchi, Y., Kameyama, T., 2005. J. Nucl. Sci. Technol. **42**, 503.

Nauchi, Y., Kameyama, T., 2010. Nucl. Sci. Technol. **47**, 977.

Nauchi, Y., 2014. In *Proceedings of the SNA+MC 2013 conference*, Paris, France.

OECD Nuclear Energy Agency, 2010. International Handbook of Criticality Safety Benchmark Experiments. Report NEA/NSC/DOC(95)03.

Ott, K. O., Neuhold, R. J., 1985. Nuclear Reactor Dynamics, Am. Nucl. Society.

Paxton, H. C., 1981. Progr. Nucl. Energy **7**, 151.

Perfetti, C. M., PhD thesis, 2012. Michigan University.

Persson, C. M., et al., 2008. Ann. Nucl. En. **35**, 2357.

Pfeiffer, W., Brown, J.R., Marshall, A.C., 1974. GA-A13079, General Atomic.

Richard, B., PhD thesis, 2013. Paris-Sud University.

Santamarina, A., Blaise, P., Erradi, L., Fougeras, P., 2012. Ann. Nucl. En. **48**, 51.

Santamarina, A., et al., 2014. In *Proceedings of the M&C 2013 Conference*, Sun Valley, USA.

Shim, H. J., Kim, C. H., Kim, Y., 2011. J. Nucl. Sci. Technol. **48**, 1453.

Sjenitzer, B.L., Hoogenboom, J.E., 2011. Ann. Nucl. Eng. **38**, 2195.

Soodak, H., 1949. Pile kinetics. In: Goodman, G. (Ed.), The Science and Engineering of Nuclear Power, vol. II. Addison-Wesley Press, Inc., Cambridge, pp. 89102.

Spanier, J., Gelbard, E. M., 1969. Monte Carlo Principles and Neutron Transport Problems. Addison-Wesley, Massachusetts, USA.

Spriggs, G. D., et al., 1997. LA-UR-97-1073, Los Alamos.

Tripoli-4 Project Team, 2012. Tripoli-4 User guide, Rapport CEA-R-6316.

Truchet, G., et al., 2014. In *Proceedings of the SNA+MC 2013 conference*, Paris, France.

Truchet, G., et al., 2014. In *Proceedings of the Physor2014 conference*, Kyoto,

445   Japan.

Ussachoff, L. N., 1955. In *Proceedings of the 1st UN conference of the peaceful uses of atomic energy*, P/503, Geneva, Switzerland.

Various authors, 1981. Rapport de Sûreté de l'INB 101 ORPHEE.

Verboomen, B., Haeck, W., Baeten, P., 2006. Ann. Nucl. En. **33**, 911.

450 Weinberg, A. M., 1952. Am. J. Phys. **20**, 401.

X-5 Monte Carlo Team, 2003. MCNP - A general Monte Carlo N-particle transport code, Version 5, Volume I: Overview and theory. LA-UR-03-1987, Los Alamos Laboratory.

Zoia, A., Dumonteil, E., Mazzolo, A., Mohamed, S., 2012. J. Phys. A: Math.
455 Theor. **45**, 425002.

Zoia, A., Dumonteil, E., Mazzolo, 2012. Europhys. Lett. **100**, 40002.

Zoia, A., Brun, E., Malvagi, F., 2014. Ann. Nucl. En. **63**, 276 (2014).

Zoia, A., Brun, E., Damian, F., Malvagi, F., 2014. Ann. Nucl. En. **75**, 627 (2014).

Configuration	Measured	T4 IFP	MCNP IFP
JEZEBEL-233	−100 ± 1	−107.15 ± 0.35	−108 ± 1
FLATTOP-23	−26.7 ± 0.5	−29.15 ± 0.2	−30.2 ± 0.4
GODIVA	−111 ± 2	−114 ± 0.59	−113 ± 1
FLATTOP-25	−38.2 ± 0.2	−39.55 ± 0.09	−39.7 ± 0.2
ZEUS-1	−0.338 ± 0.008	−0.36 ± 0.008	−0.363 ± 0.002
ZEUS-5	−7.96 ± 0.08	−10.81 ± 0.03	−10.76 ± 0.07
ZEUS-6	−3.73 ± 0.05	−4.07 ± 0.01	−4.14 ± 0.03
BIGTEN	−11.7 ± 0.1	−11.8 ± 0.03	−11.8 ± 0.1
STACY-30	−0.0127 ± 0.0003	−0.01273 ± 0.0001	−0.0133 ± 0.0003
STACY-46	−0.0106 ± 0.0004	−0.01080 ± 0.0001	−0.0104 ± 0.0002
JEZEBEL	−64 ± 1	−63.83 ± 0.37	−65 ± 1
FLATTOP-PU	−21.4 ± 0.5	−21.34 ± 0.16	−21.0 ± 0.3
THOR	−19 ± 1	−21.48 ± 0.35	−20 ± 1

Table 3: The parameter α_{Rossi} (in units of 10^4 s^{-1}) for the reactor configurations of the Rossi alpha validation suite. We compare the measured α_{Rossi} to the values computed by TRIPOLI-4 ® by resorting to the ENDF/B-VII.0 nuclear data library. For reference, the values computed by MCNP with the same nuclear data library are also displayed.

Configuration	Measured	T4 IFP	MCNP IFP	T4 NFP	T4 β_0
JEZEBEL-233	289 ± 7	294 ± 1	296 ± 2	292 ± 0.3	281 ± 0.2
FLATTOP-23	360 ± 9	371 ± 2	383 ± 5	337 ± 0.6	578 ± 0.5
GODIVA	645 ± 13	649 ± 3	644 ± 7	644 ± 0.9	641 ± 0.5
FLATTOP-25	665 ± 4	689 ± 2	692 ± 3	621 ± 0.4	812 ± 0.3
BIGTEN	720 ± 7	725 ± 2	725 ± 4	705 ± 0.1	910 ± 0.4
JEZEBEL	190 ± 4	183 ± 1	187 ± 2	183 ± 0.3	204 ± 0.2
FLATTOP-PU	276 ± 7	283 ± 2	279 ± 4	257 ± 0.5	537 ± 0.5

Table 4: The delayed neutron fraction β_{eff} (pcm) for the reactor configurations of the Rossi alpha validation suite. We compare the measured β_{eff} to the values computed by TRIPOLI-4 ® by resorting to the ENDF/B-VII.0 nuclear data library. For reference, the values computed by MCNP with the same nuclear data library are also displayed. Moreover, we show the β_{eff} estimated by the NFP method and the un-weighted average delayed neutron fraction β_0, as computed by TRIPOLI-4 ®.

Configuration	Computed	T4 IFP	MCNP IFP	T4 NFP	T4 Λ_0	MCNP T_0/k_{eff}
JEZEBEL-233	2.9	2.75 ± 0.0008	2.74 ± 0.0016	2.79 ± 0.0004	3.21 ± 0.00013	3.21 ± 0.00012
FLATTOP-23	13.5	12.7 ± 0.017	12.7 ± 0.03	15.1 ± 0.0.0048	71.9 ± 0.008	71.7 ± 0.0065
GODIVA	5.8	5.69 ± 0.0037	5.70 ± 0.0075	5.72 ± 0.0011	6.25 ± 0.0003	6.24 ± 0.00052
FLATTOP-25	17.5	17.4 ± 0.0085	17.4 ± 0.017	18.8 ± 0.0023	66.6 ± 0.003	66.5 ± 0.0026
BIGTEN	62	61.5 ± 0.024	61.5 ± 0.05	62.4 ± 0.006	112 ± 0.006	111 ± 0.0053
JEZEBEL	3	2.87 ± 0.0012	2.87 ± 0.0025	2.92 ± 0.0004	3.74 ± 0.0002	3.74 ± 0.00021
FLATTOP-PU	12.9	13.3 ± 0.017	13.3 ± 0.003	15.7 ± 0.0046	77.5 ± 0.009	77.3 ± 0.0065

Table 5: The mean generation time Λ_{eff} (in units of 10^{-9} s) for the reactor configurations of the Rossi alpha validation suite. We compare the computed $\Lambda_{\text{eff}} = -\beta_{\text{eff}}/\alpha_{\text{Rossi}}$ to the values computed by TRIPOLI-4 ® by resorting to the ENDF/B-VII.0 nuclear data library. For reference, the values computed by MCNP with the same nuclear data library are also displayed. Moreover, we show the Λ_{eff} estimated by the NFP method and the un-weighted mean generation time Λ_0, as computed by TRIPOLI-4 ®. The parameter Λ_0 is compared to the value T_0/k_{eff} computed by MCNP with the same nuclear data library.

Configuration	Measure	T4 IFP	AP-2	T4 NFP	T4 β_0
MISTRAL1	788 ± 12	797 ± 3	792	784 ± 1	716 ± 1
MISTRAL2	370 ± 6	372 ± 3	371	368 ± 1	355 ± 1

Table 6: The delayed neutron fraction β_{eff} (pcm) for the reactor configurations MISTRAL1 and MISTRAL2. We compare the measured β_{eff} to the values computed by TRIPOLI-4 ® by resorting to the JEFF3.1.1 nuclear data library. For reference, the values computed by the APOLLO-2 deterministic code using the SHEM-MOC calculation scheme with the same nuclear data library are also displayed. Moreover, we show the β_{eff} estimated by the NFP method and the un-weighted average delayed neutron fraction β_0, as computed by TRIPOLI-4 ®.

Configuration	Measured	T4 IFP ENDF/B-VII.0	T4 IFP JEFF3.1.1
JEZEBEL-233	-100 ± 1	-107.15 ± 0.35	-110 ± 0.36
FLATTOP-23	-26.7 ± 0.5	-29.15 ± 0.2	-30.4 ± 0.2
GODIVA	-111 ± 2	-114 ± 0.59	-113 ± 0.57
FLATTOP-25	-38.2 ± 0.2	-39.55 ± 0.09	-40 ± 0.09
ZEUS-1	-0.338 ± 0.008	-0.36 ± 0.008	-0.37 ± 0.008
ZEUS-5	-7.96 ± 0.08	-10.81 ± 0.03	-10.63 ± 0.03
ZEUS-6	-3.73 ± 0.05	-4.07 ± 0.01	-4.07 ± 0.01
BIGTEN	-11.7 ± 0.1	-11.8 ± 0.03	-11.9 ± 0.03
STACY-30	-0.0127 ± 0.0003	-0.01273 ± 0.0001	-0.013 ± 0.0001
STACY-46	-0.0106 ± 0.0004	-0.01080 ± 0.0001	-0.0109 ± 0.00008
JEZEBEL	-64 ± 1	-63.83 ± 0.37	-67 ± 0.38
FLATTOP-PU	-21.4 ± 0.5	-21.34 ± 0.16	-22.3 ± 0.17
THOR	-19 ± 1	-21.48 ± 0.35	-20.65 ± 0.35

Table 7: The parameter α_{Rossi} (in units of 10^4 s^{-1}) for the reactor configurations of the Rossi alpha validation suite. We compare the experimental measurements to the values computed by TRIPOLI-4 ® by resorting to the ENDF/B-VII.0 or JEFF3.1.1 nuclear data libraries.

Configuration	Measured	T4 IFP ENDF/B-VII.0	T4 IFP JEFF3.1.1
JEZEBEL-233	289 ± 7	294 ± 1	292 ± 1
FLATTOP-23	360 ± 9	371 ± 2	377 ± 2
GODIVA	645 ± 13	649 ± 3	646 ± 3
FLATTOP-25	665 ± 4	689 ± 2	694 ± 2
BIGTEN	720 ± 7	725 ± 2	739 ± 2
JEZEBEL	190 ± 4	183 ± 1	188 ± 1
FLATTOP-PU	276 ± 7	283 ± 2	290 ± 2

Table 8: The delayed neutron fraction β_{eff} (pcm) for the reactor configurations of the Rossi alpha validation suite. We compare the experimental measurements to the values computed by TRIPOLI-4 ® by resorting to the ENDF/B-VII.0 or JEFF3.1.1 nuclear data libraries.

Configuration	Computed	T4 IFP ENDF/B-VII.0	T4 IFP JEFF3.1.1
JEZEBEL-233	2.9	2.75 ± 0.0008	2.66 ± 0.00076
FLATTOP-23	13.5	12.7 ± 0.017	12.4 ± 0.016
GODIVA	5.8	5.69 ± 0.0037	5.71 ± 0.0036
FLATTOP-25	17.5	17.4 ± 0.0085	17.4 ± 0.0082
BIGTEN	62	61.5 ± 0.024	62.1 ± 0.025
JEZEBEL	3	2.87 ± 0.0012	2.81 ± 0.0011
FLATTOP-PU	12.9	13.3 ± 0.017	13.0 ± 0.0017

Table 9: The mean generation time Λ_{eff} (in units of 10^{-9} s) for the reactor configurations of the Rossi alpha validation suite. We compare the computed $\Lambda_{\text{eff}} = -\beta_{\text{eff}}/\alpha_{\text{Rossi}}$ to the values computed by TRIPOLI-4 ® by resorting to the ENDF/B-VII.0 or JEFF3.1.1 nuclear data libraries.